GRAIN GROWTH

IN

POLYCRYSTALLINE MATERIALS

Proceedings of the 1st International Conference on
Grain Growth in Polycrystalline Materials, held in Rome, Italy, 18-21 June, 19

Edited by

G. ABBRUZZESE and P. BROZZO

Centro Sviluppo Materiali

TRANS TECH PUBLICATIONS
Switzerland - Germany - UK - USA

Materials Science Forum Vols. 94-96 (1992) pp. 39-52

COMPARISON OF SOAP FROTH AND SIMULATION OF LARGE-Q POTTS MODEL

S. Ling, M.P. Anderson and G.S. Grest (a) and
J.A. Glazier (b)
(a) Corporate Research Science Laboratory, Exxon Research and Engineering Co., Annandale, NJ 08801, USA
(b) AT&T Bell Laboratories, Murray Hill NJ 07974, USA

ABSTRACT

The temporal evolution of a two-dimensional soap froth is compared to the predictions of the large Q-state Potts model computer simulation. This study was conducted using identical initial states in both the experiment and Potts model. Overall agreement is found between the soap froth and the large Q Potts model results with respect to pattern evolution, dynamics, distribution functions, and topological correlations.

1. INTRODUCTION

The complete prediction of microstructural development in polycrystalline solids as a function of time is a major objective in materials science.[1, 2, 3] Progress in this area has been quite slow owing to the complexity of the grain interactions. While a general analytical solution is not yet available, two powerful methodologies have been successfully applied to the investigation of this multivariable problem. The first one is the computer simulation based on the Potts model.[4, 5, 6, 7, 8, 9, 10, 11] This approach has successfully incorporated many aspects of the grain interactions and can predict the

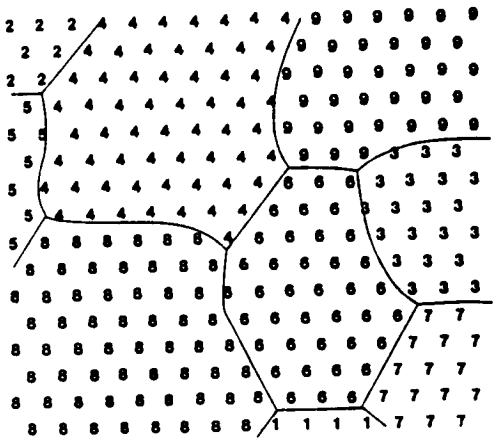

Figure 1: A polycrystalline microstructure is discretized with a triangular lattice. The integral spin numbers denote crystallographic orientations, and the lines represent grain boundaries.

main features of the microstructural temporal evolution. The other methodologyis the two-dimensional soap froth experiment first proposed by Smith for studying grain growth phenomena.[12] Using this approach Stavans *et al* demonstrated that the dynamics of the soap bubble evolution obeys the von Neumann's law.[13, 14] In this paper we review some of our recent work in comparing the similarities and differences between the soap froth experiment and the two-dimensional large-Q Potts model in simulating the evolution of two-dimensional polycrystalline microstructure under grain growth conditions.[15]

2. METHODOLOGY

2.1 Potts model based on Monte Carlo technique

The polycrystalline microstructure is mapped onto a lattice. In two-dimension this lattice can be either square or triangular (see figure **1**). To each site is assigned a spin number, $S_i : 1 \leq S_i \leq Q$, that denotes the orientation of the grain in which the site is embedded. Here Q is the largest spin number used in the lattice. The total Hamiltonian for this spin system is defined as:[11]

$$H = J \sum_i \sum_j (1 - \delta_{S_i S_j}) \qquad (1)$$

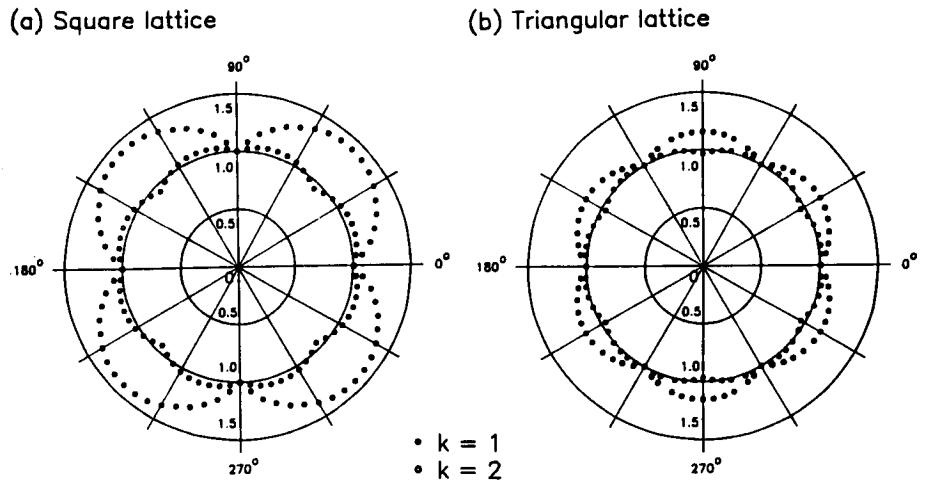

Figure 2: Wulff plots showing the energy of unit length grain boundary with respect to the underlying lattice, for both nearest ($k = 1$) and next-nearest neighbor ($k = 2$) interactions. The energies are normalized to unity in the 0° direction. (a) square, and (b) triangular-lattices.

where J is a positive constant related to the grain boundary energy, δ_{ab} is the Kronecker delta function, $\sum_j$ is summed over all sites within the kth nearest neighbor shell of the i site, which is in turn summed over all sites in the lattice with $\sum_i$.

Depending on the particular lattice used, the Hamiltonian in equation 1 exhibit orientational anisotropy as shown in figure 2, which are the Wulff plots for the square and triangular lattices. These are the polar plots of grain boundary energies in different orientations. The energies are all normalized to have unit magnitude in the 0° direction. The actual magnitude of the energies in the 0° direction, for the square and triangular lattices respectively, are J and $2J$ for $k = 1$, and $3J$ and $4J$ for $k = 2$. It can be seen that the square lattice exhibit strong anisotropy when only the nearest neighbor interaction is considered. Since an anisotropic Hamiltonian reduces the effective force driving boundary motion,[16] we therefore work with the $k = 1$ triangular, and $k = 2$ square lattices.

The kinetics of boundary migration are simulated using a Monte Carlo technique in which a site, selected at random, is reoriented to a randomly chosen new orientation. In the zero temperature regime, this reorientation

attempt is accepted only if the resulting energy is less than or equal to zero. A time of one Monte Carlo Step (MCS) corresponds to a number of reorientation attempts equal to the number of lattice sites.

2.2 Soap froth experiment

A cell of 8.5 *in.*×11.5 *in.*×1/8 *in.* is used.[17] Employing air as working gas, the cell is filled with a well ordered array of small bubbles, which typically numbered in the range of 10,000 initially. The 1/8 *in.* thickness of the cell is adequately small that the bubbles are in contact with both the top and bottom plates, resulting in a two-dimensional bubble network resembling polycrystalline grain structure. The top and bottom plates are made of clear plastic which allows the use of a photocopier to record the coarsening of the grain structure as a function of time. The soap froth images were digitized using an IBAS image analyzer, such that the same 30% area of every image is resolved into 600×500 pixels on a square lattice. The resulting digitized images were then subjected to further statistical analysis.

2.3 Potts simulations and soap froth experiment using identical initial states

Two types of Potts model simulations were conducted: the $k = 1$ triangular lattice simulation for gathering statistics in the power law regime (also called the scaling state), and the $k = 2$ square lattice simulation to provide comparisons to the soap froth experiment.[15] For compatibility reasons, the simulations were carried out using two-dimensional lattices. The triangular lattice simulation used $Q = 48$ on a 1000×1000 lattice having periodic boundary conditions. The square lattice simulation, on the other hand, used $Q = Q_{max}$ on a 600×500 lattice having open boundary condition (*i.e.* spins on the border were assumed to interact with frozen impurities). Here Q_{max} equals the number of grains in the initial state. In doing the analysis, any grains (or bubbles in the case of soap froth) touching the borders are excluded from the statistics. This is to reduce the effect on our analysis of the different boundary conditions used in the soap froth and the Potts model simulations.

3. RESULTS AND DISCUSSIONS

3.1 Evolution and statistics of the grain structures

Figure **3** shows the evolution of the structures observed in the soap froth (30% detail) as well as that obtained from the square lattice Potts simulations. As can be seen in the froth, the $t = 0$ *min.* pattern is composed almost entirely of small and ordered hexagonal grains of nearly equal areas, whereas the $t = 2044$ *min.* pattern has evolved to a state in which a few islands of these six-sided grains still remain. Two square lattice Potts model simulations were carried out, employing as their respective initial states the digitized froth images at $t = 0$ *min.* ($Q_{max} = 2490$) and $t = 2044$ *min.* ($Q_{max} = 1175$). The qualitative features of the disordering observed in the froth is similar to that found in the simulations.

A clear difference between these patterns of the two methodologies, however, is the angles at which the grains boundaries meet the border. In the case of the Potts model, this angle is close to 90°. This is due to the fact that open boundary conditions were used in the simulation. In the case of the soap froth, the same boundaries cross the border at arbitrary angles. It should be noted that the border in the case of the soap froth merely defines the extent of the viewing window, which covers 30% of the whole cell surface area. Consequently the border does not have actual physical interaction with the grain structure. This difference in the boundary conditions results in an increasing divergence with time between the patterns of the actual soap froth and the simulations, as can be seen by comparing the bottom row simulation structures to the corresponding froth image in figure **3**.

Figure **4** shows the average grain size as a function of time, which is compared between the froth and two triangular lattice Potts simulations using different initial states. Since these initial states were both taken from images of the same soap froth cell, there was no free parameter exist in assigning grain areas (measured in pixels) in the Potts simulations. The multiplicative constant relating the real time to the Monte Carlo steps, however, is a free parameter. This was chosen to give the best fit to the $t = 2044$ *min.* run, so that $t_{real}\ (min) = 0.32 t_{MC} + 2044$, where t_{MC} is the number of Monte Carlo Steps (MCS).

Based upon this best fit, it can be seen that all three sets of data exhibit a slow initial growth, followed by a rapid transient, then a slower, approxi-

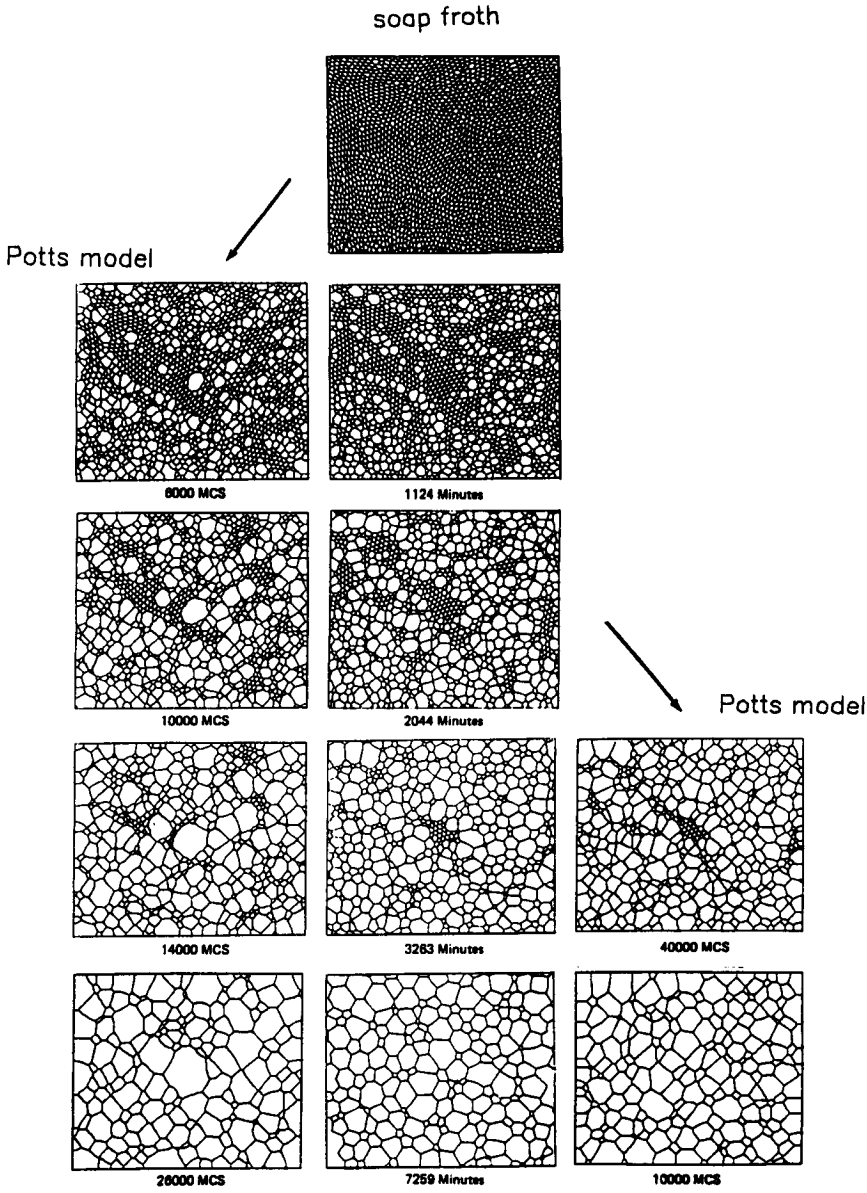

Figure 3: Comparison of the two-dimension structures of soap froth (center) and Potts model simulations. The simulations use as their respective initial states the digitized froth images at $t = 0$ *min.* (left) and $t = 2044$ *min.* (right).

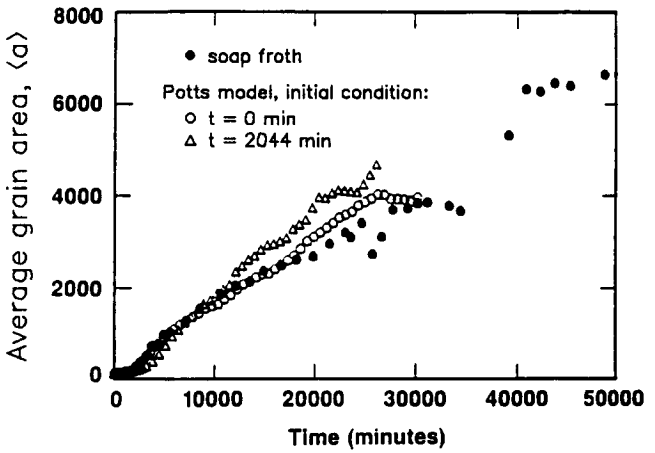

Figure 4: Comparison of average grain area (in pixels) as function of time.

mately power-law growth behavior in which the average grain area is a linear function of time.[17] After this the data show fluctuations. The early transient in the froth is attributed to the annealing out of the initial fill state of small ordered grains. It can also be seen from figure 4 that the soap froth is faster than the Potts simulations in increasing its grain sizes in the initial transient, as well as quicker in entering a power law regime (or scaling state). This suggests that the initial cluster of small hexagonal grains are more stable in the Potts simulations than the corresponding bubbles in the soap froth. We believe that this is a manifestation of the finite size effect, caused by the fact that the initial short time grain size in the simulation is not much larger than the lattice separation of the underlying grid.

In the scaling state, the grain statistics and various distributions are found to be time invariant. Figure 5 compares the distributions of normalized grain radius and area obtained from the soap froth, as well as Potts simulation using a triangular lattice. Both curves display similar behavior. The radius plot in figure **5(a)** shows that the simulation results in more grains of average size (*i.e.* $r/ < r >= 1$, where $< >$ indicates mean value) than that of the soap froth. In the area plot, figure **5(b)**, both curves exhibit a monotonic exponential decrease.

3.2 Topological statistics

The topological state of a grain structure can be described by the side distribution function, $\rho(n)$, which gives the probability that a randomly selected

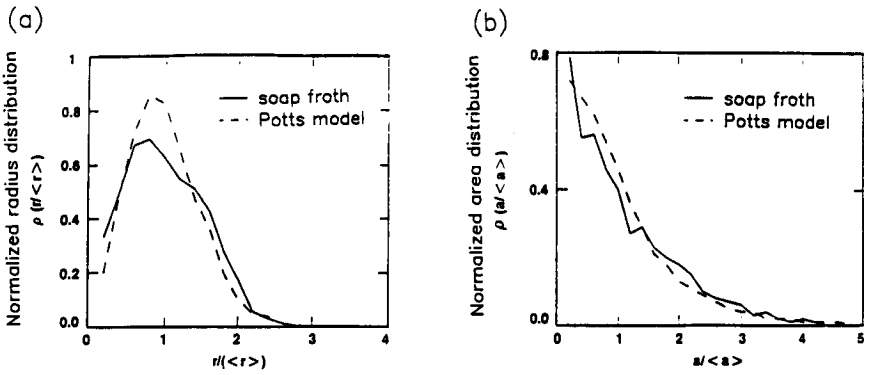

Figure 5: Scaling state plot of (a) normalized radius distribution, and (b) normalized area distribution.

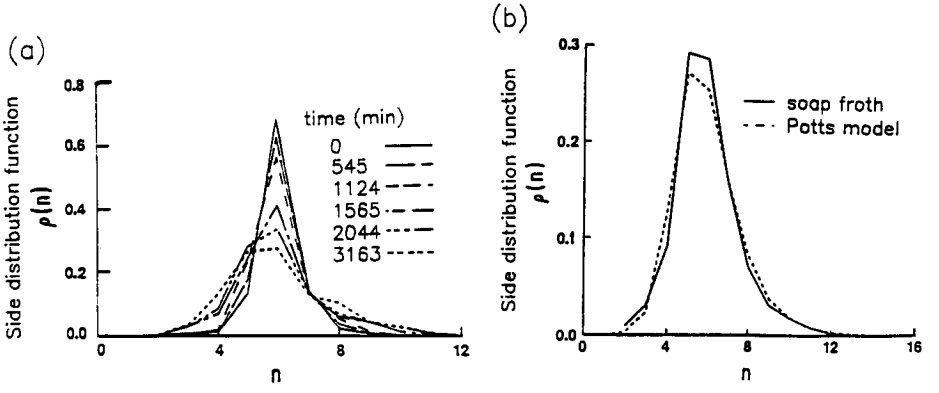

Figure 6: Side distribution function, $\rho(n)$: (a) plotted at different times for an initially ordered froth, and (b) in scaling state, comparison between the soap froth and a Potts simulation using triangular lattice.

grain has n sides. Figure **6(a)** shows the evolution of the side distribution for the soap froth in figure **3**. At $t = 0$ *min.*, the function sharply peaks at $n = 6$, because the structure starts out as a well ordered arrays of hexagonal grains. With increasing time, $\rho(6)$ of six-sided grains is found to decreases monotonically, whereas $\rho(5)$ of five-sided grains increases monotonically. After approximately $10,000$ *min.*, at which point the system achieves the scaling state, the shape of the distribution function becomes essentially time invariant, and $\rho(5)/\rho(6) = 1.03$. This observation agrees with the earlier finding by Stavans *et al.*[14] In figure **6(b)**, the scaling state side distributions are plotted for the froth and a Potts simulation using the triangular lattice. It can be seen here that the froth curve shows more five- and six-sided grains, whereas the simulation curve has more four- and eight-sided grains.

In order to better visualize the temporal development of the grain topology, we define the mth moment of $\rho(n)$:

$$\mu_m = \sum_{n=2}^{\infty} \rho(n)(n - < n >)^m \tag{2}$$

where $< n >$ is the average number of sides for a grain in the structure. In figure **7** we plot μ_2, which measures the r.m.s. width of the distribution, against time for the soap froth and the $t = 0$ *min.* square lattice Potts simulation. The scatter of data is attributed to the limited number of observable grains due to the restricted size of the digitized images. It can be seen that both curves display essentially the same pattern. At $t = 0$, we observe low μ_2 values which is due to the presence of large number of hexagonal grains, that gives rise to a sharp side distribution functions, $\rho(n)$. In the transient state, the μ_2's grow rapidly, indicating the broadening of $\rho(n)$. Here it can be seen that the μ_2 of the Potts model grows at a slower rate, but eventually reaches a higher value, than that of the froth. The systems enter the scaling state at about $t = 10,000$ *min.*, at which point the μ_2's drop back to more stable values ($\mu_2 = 1.5 \pm 0.3$ for froth, and 2.4 ± 0.1 for Potts model). These stable μ_2 values indicate time invariant side distributions.

We next examine the relationship between grain size and topology. Two different forms concerning cellular type arrays have been proposed. The first form is the commonly used Lewis' law,[18] in which the area of a grain is assumed to be a linear function of its number of sides: $< a_n > = c_1 + c_2 n$, where $< a_n >$ is the mean area of the grains having n-sides, and c_1, c_2 are

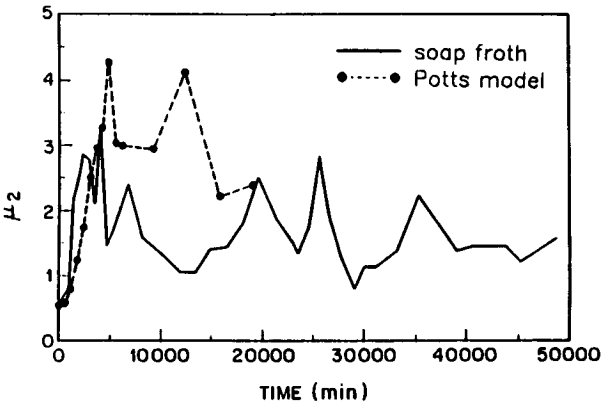

Figure 7: Time evolution of second moment of the side distribution, μ_2, for the soap froth and the square lattice Potts model simulation using as initial condition $t = 0$ *min.* froth image.

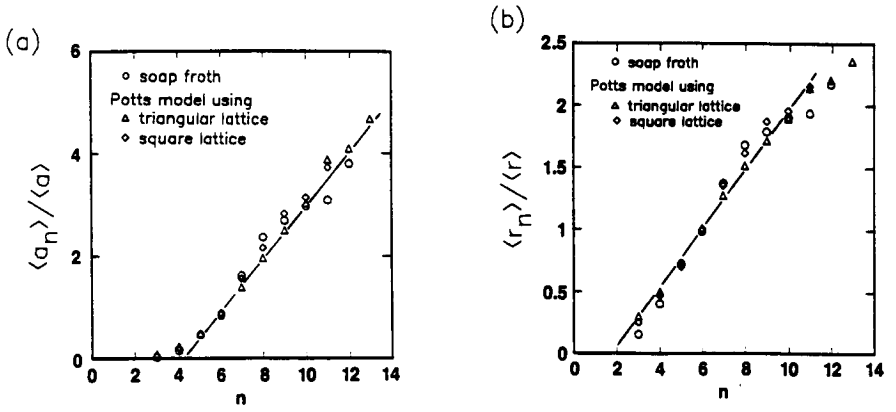

Figure 8: Plot of (a) normalized average area of n-sided grains versus n. The line shows Lewis' law prediction. (b) normalized average radius of n-sided grains versus n. The line shows Feltham's law prediction.

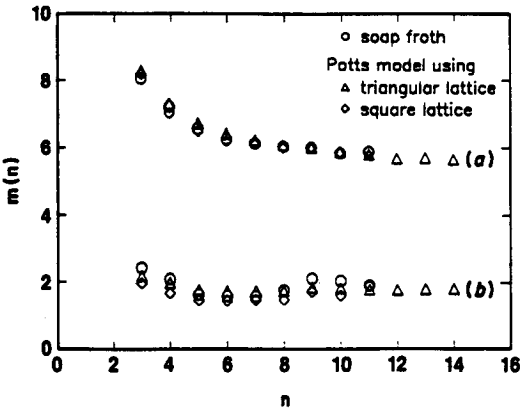

Figure 9: (a) Nearest neighbor side correlation function, $m(n)$, and (b) its standard deviation. Both are plotted as function of n, the number of grain sides.

constants. Figure 8(a) plots the normalized grain area as function of n for the soap froth and Potts simulations, both square and triangular lattices runs. The three results are indistinguishable within numerical uncertainty, and all display a non-linear relationship. In particular, the areas of the grains having fewer than six sides appear to be larger than that predicted by the Lewis' law.

The second form is the Feltham's law,[19] in which the size of a grain is assumed to be a linear function of its number of sides: $< r_n > = c_1 + c_2 n$, where $< r_n >$ is the mean radius of the grains having n-sides. Figure 8(b) plots the normalized grain radius as function of n. Again we see that all three results are in good agreement with each other. In this case, however, the radius of the grains having more than ten sides appear to be lower than that predicted by the Feltham's law.

Another important topological distribution that can be readily calculated is the nearest neighbor side correlation function, $m(n)$, which is the average-number-of-sides of the neighboring grains to an n-sided grain, $m(n)$.[20] This function can be expressed in a form first proposed by Weaire: $m(n) = k_1 + c/n$, and is known as the Aboav-Weaire law.[21] Figure 9 presents the function $m(n)$ and its standard errors, obtained from the soap froth as well as the Potts simulations. The three data sets are in good agreement with each other, as well as with the Aboav-Weaire Law. They all show a monotonic decrease, especially between $n = 3$ and 8. This indicates that few-sided

grains tend to be near many-sided grains.

4. SUMMARY

It is found that the Potts model and the soap froth experiment show excellent agreement, and they produce nearly identical distribution and correlation functions. There are, however, a few subtle discrepancies. In the early time behavior, the hexagonal grains in the Potts model are found to be more stable than those in the soap froth. This effect is believed to be a manifestation of the finite size effect. Also in the side distribution during the scaling state, the longer tail of the Potts model shows that its many-sided grains lose sides more slowly than those in the soap froth, and presumably gain sides more frequently. At this moment it is not clear if these discrepancies are specific to the methodologies employed, or are the manifestation of some more fundamental underlying issues. Further investigation would be necessary to answer this question.

References

[1] P.A. Beck, *Adv. Phys.*, **3**, p. 245 (1954).

[2] R.V. Randle, B. Ralph, and N. Hansen, in *Annealing Processes — Recovery, Recrystallization and Grain Growth, Proceedings of the Seventh Risø International Symposium on Metallurgy and Materials Science*, ed. Hansen, N., Juul Jensen, D., Leffers, T., and Ralph, B., p. 123 (Risø: Risø National Laboratory, 1986).

[3] H.V. Atkinson: *Acta metall.*, 1988, **36**, p. 469.

[4] M.P. Anderson, D.J. Srolovitz, G.S. Grest, and P.S. Sahni: *Acta metall.*, 1984, **32**, p. 783.

[5] D.J. Srolovitz, M.P. Anderson, G.S. Grest, and P.S. Sahni: *Act metall.*, 1984, **32**, p. 1429.

[6] D.J. Srolovitz, G.S. Grest, P.S. Sahni, and M.P. Anderson: *Act metall.*, 1984, **32**, p. 793.

[7] G.S. Grest, D.J. Srolovitz, M.P. Anderson: *Acta metall.*, 1985, **33**, p. 509.

[8] M.P. Anderson, G.S. Grest, and D.J. Srolovitz: in *Computer Simulation of Microstructural Evolution*, ed. Srolovitz, D.J., pp. 77–93 (Warrendale, Pennsylvania, Metallurgical Society of AIME, 1986).

[9] G.S. Grest, D.J. Srolovitz, and M.P. Anderson: in *Computer Simulation of Microstructural Evolution*, ed. Srolovitz, D.J., pp. 21–32 (Warrendale, Pennsylvania, Metallurgical Society of AIME, 1986).

[10] G.S. Grest, D.J. Srolovitz, M.P. Anderson: *Phys. Rev.* B, 1988, **38**, p. 4752.

[11] M.P. Anderson, G.S. Grest: *Phil. Mag.* B, 1989, **59**, [3], pp. 293–329.

[12] C.S. Smith: in *Metal Interfaces*, pp. 65–108 (Cleveland, Ohio, American Society for Metals, 1952).

[13] J. von Neumann: in *Metal Interfaces*, pp. 108–110 (Cleveland, Ohio: American Society for Metals, 1952).

[14] J. Stavans and J.A. Glazier: *Phys. Rev. Lett.*, 1989, **62**, p. 1318.

[15] J.A. Glazier, M.P. Anderson, and G.S. Grest: *Phil. Mag.* B, 1990, **62**, [6], pp. 615-645.

[16] E.A. Holm, J.A. Glazier, D.J. Srolovitz, and G.S. Grest: *Phys. Rev.* A, 1991, **43**, [6], pp. 2662–2668.

[17] J.A. Glazier, S.P. Gross, and J. Stavans: *Phys. Rev.* A, 1987, **36**, p. 306.

[18] F.T. Lewis: *Anat. Rec.*, 1928, **38**, p. 341 .

[19] P. Feltham: *Acta metall.*, 1957, **5**, p. 97.

[20] D.A. Aboav: *Metallography*, 1970, **3**, p. 383.

[21] C.J. Lambert, and D. Weaire: *Metallography*, 1981, **14**, p. 307; *Phil. Mag.* B, 1983, **47**, p. 445.